International Journal of Control, Automation, and Systems 21(6) (2023) 1950-1958
http://dx.doi.org/10.1007/s12555-021-1001-4
ISSN:1598-6446 eISSN:2005-4092
http://www.springer.com/12555

Whole-body Control Based Lifting Assistance Simulation for Exoskeletons

Jeonguk Kang, Donghyun Kim, Hyun-Joon Chung, Kwang-Woo Jeon, and Kyung-Soo Kim*

Abstract: Exoskeletons can help humans in a variety of ways in performing tasks. In particular, during the lifting operation, a human places a great burden on the knee or waist joint, and the exoskeleton can reduce the risks of this task. However, due to the weight of the exoskeleton itself and the movement of the overall center of gravity, balance ability and efficiency may decrease. Therefore, an appropriate assistance torque distribution strategy is required to achieve high performance with the exoskeleton. In order to solve the aforementioned problem, we propose an assistance method based on whole-body control. The proposed algorithm is meaningful because it is different from other simple model-based controllers. The controller fully utilize the dynamics to achieve a high performance. In addition, by adding a straight leg cost term, the singularity problem in the fully extended configuration was solved. This method finds the optimal solution that satisfies various constraints and minimizes the objective functions. Each objective is composed of a balancing-related term that minimizes the variation in the center of gravity, a term that supports the weight of the human and exoskeleton, a term that solves the singularity problem and a term related to efficiency. In this paper, first, a motion capture experiment is performed to analyze a human's lifting motion. Through this experiment, the trajectory of each joint angle is obtained. With PD (proportional–derivative) feedback from the joint trajectories, the exoskeleton generates human torque in the simulation and implements a lifting operation. Second, a simulation is performed with the proposed controller. As a result, it is confirmed that the proposed method reduces the amount of human joint torque and increases stability and efficiency.

Keywords: Exoskeleton, squat lifting, wearable robotics, whole-body control.

1. INTRODUCTION

In the industrial field, there are many simple and repetitive tasks. Among them, movements of lifting and lowering objects increases the risk of back and knee injuries. Therefore, several research groups have developed passive and active exoskeletons over the past decade to reduce injuries during lifting. First, the passive exoskeleton based on a spring or elastic-based material was studied [1,2]. It was designed to use the stored energy that is generated when the joint is in maximum flexion. Since no actuator is used, it is relatively lightweight and does not need additional controllers. Its effects and performance have been studied with various results [3-5]. However, there is a drawback that it showed limited performance only for certain movements and cannot actively apply assistance torque. In contrast, with an active exoskeleton, assistance torque can be actively applied depending on the situation, but the overall system weight becomes heavier, which also causes imbalance.

Because a large moment occurs at the lowest point, active exoskeleton studies have mainly focused on knee support [6,7]. Therefore, these studies suggest a method of assisting only the knee joint. Next, exoskeletons and control techniques that support the ankle or waist have been also developed [8]. Since this assistance force has additional effects on other joints by action and reaction, each torque must be properly distributed. In order to maximize the performance of the active exoskeleton, the control system should be constructed appropriately for the task, and interaction with people should be considered. Research on assistance torque generation has been studied in various directions, from position based trajectory control to model based control. For model based control, authors of [9] controlled the exoskeleton through nonlinear model predictive control, and authors of [10] controlled impedance by es-

Manuscript received November 26, 2021; revised June 1, 2022 and August 22, 2022; accepted October 31, 2022. Recommended by Associate Editor Maolin Jin under the direction of Senior Editor Kyoung Kwan Ahn. This research was financially supported by the Institute of Civil Military Technology Cooperation and funded by the Defense Acquisition Program Administration and Ministry of Trade, Industry and Energy of the Korean government under grant No. 19-CM-GU-01. Jeonguk Kang and Donghyun Kim are co-first authors.

Jeonguk Kang, Donghyun Kim, and Kyung-Soo Kim are with the Department of Mechanical Engineering, Korea Advanced Institute of Science and Technology, Daejeon 34141, Korea (e-mails: {kju2556, kdh6719, kyungsookim}@kaist.ac.kr). Hyun-Joon Chung and Kwang-Woo Jeon are with the Korea Institute of Robotics and Technology Convergence, Pohang 37666, Korea (e-mails: {hjchung, jeonkw}@kiro.re.kr).
* Corresponding author.

timating human torque for a paralyzed patient. Recently, with the development of AI, reinforcement learning-based research has been actively conducted [11].

The controller proposed in this paper is a whole-body control based method. It has been mainly used in robotics, and it is a method to find an optimal solution that is suitable for multiple tasks simultaneously [12,13]. Unlike model predictive control, which considers the long term, whole-body controller has the advantage of obtaining an optimized value at every moment. Additionally, it can easily configure multiple tasks and determine their importance. This kind of controller has been studied for various purposes. For example, in [14], optimization problems were solved sequentially according to their priority using the hierarchical optimization method, and in [15], an internal force control method was introduced for the case in which the system is an under-actuated condition. The method of [16] was used in a quadruped robot, whole-body impulse control was introduced to effectively generate the ground reaction force, which is a high-level command, and this maximized the performance. These studies were mainly applied to legged motion control, and the same approach could be applied to lifting because of the similar configuration.

The main contribution of this paper is to maximize the exoskeleton lifting performance by applying a numerical whole-body controller considering straight leg term. The motion of each joint and the ground reaction force were controlled through the algorithm. Due to the characteristics of the force-based controller, it could also possible to deal with disturbances. The quadratic program solver in the controller satisfies multiple tasks at the same time, and each cost function is simply added. This means we can easily add another cost functions related to other tasks. Lastly, the straight leg term in the proposed method solves the singularity problem of the general force-based controllers. This ensures reliable torque distribution even in the fully extended configuration during lifting operations. Except for using the concurrent whole-body controller in study [21], there had been no case of applying the whole-body control framework to an exo-system before. Also, unlike study [21], we solve the singularity problem in the upright configuration.

This paper is organized as follows: Section 2 introduces human body dynamics and lifting motions analyzed with motion capture cameras for simulation. Section 3 introduces how the proposed method controls the exoskeleton through the whole-body control framework. In Section 4, simulations are conducted to verify the proposed method, and the torque values and energy efficiency of each joint are analyzed. Finally, Section 5 presents a conclusion and future works.

2. HUMAN LIFTING MOTION GENERATION

2.1. Human dynamics

Human body models that perform various tasks are typically represented by 12 DOF(degrees of freedom). However, the lifting motion can be approximated in 2-dimensional space by ignoring the roll and yaw motions. In [17], the human body was described with a three-link model and a four-link model according to each task. In the case of [18], the model of the lifting motion was expressed with 6 degrees of freedom (7-link model).

If the neck is fixed to the upper body, modeling becomes possible as shown in Fig. 1. The represented figure is composed of a 6-link model, and the links are composed of a foot, shank, thigh, trunk, arm and forearm. The lifting motion can be expressed with this model configuration.

Meanwhile, the height and weight of people who wear exoskeletons are differ from person to person. That is, a human body model must be constructed with different physical quantities for each individual. In [19], each part of a human is expressed as a link based on the experiments. The mass, inertia, and center of mass of each link are obtained. This can be parameterized according to height and weight, and it can be expressed as in Table 1. Based on Table 1, an adaptive model for each experimenter is constructed. It could be used adaptively for each individual experimenter.

Finally, we need to obtain the dynamic matrix of the model. In this paper, the matrix is obtained by the La-

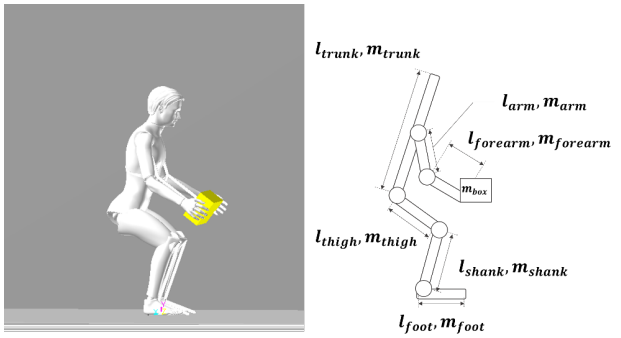

Fig. 1. A 6-link human model for the lifting motion.

Table 1. Human body distribution rate.

	Length (%)	Mass (%)
Head and neck	12.51	7.34
Trunk	32.15	47.76
Upper arm	21.47	3.34
Forearm	17.64	1.87
Hand	11.98	0.87
Thigh	26.45	11.56
Shank	25.31	4.52
Foot	3.54	1.89

grangian method, and the resulting equation of motion is expressed in the form of a matrix such as (1). M is the mass matrix, b is the Coriolis and g is the gravitational term, S is the selection matrix, J_c^T is the contact Jacobian and $b\rho$ $(= F)$ represents the ground forces. Where B is the Jacobian matrix from the generalized frame to the centroidal frame and ρ is the generalized forces.

$$M\dot{v}_d + b + g = S^T\tau + J_c^T B\rho. \quad (1)$$

2.2. Motion capture experiments

We used the Vicon motion capture system to analyze human movement. The system consists of eight Vicon T-40 cameras, and data were collected via a giganet controller and transferred to a PC. Since the lifting motion is slow, we set the camera's frame rate to 100 Hz. To analyze the experimental results, the length of each subject's body parts were measured, and markers were attached to the upper and lower extremities. The markers in the lower extremities were attached to the pelvis, thigh, knee, calf, ankle, and back of the foot. In the case of the upper extremities, they were attached to the clavicle, calf, cervical spine, lumbar spine, shoulder girdle, shoulder, elbow, wrist, and back of the hand. Each marker attachment configuration is shown in Fig. 2.

The lifting process started in a standing configuration. Then, the subject would sit in a half-squatting position and stand up holding the barbell plate. Experiments were conducted with barbells of various weights, but the task used in this paper only considered 12.5 kg, 15.0 kg, and 17.5 kg barbells. We summarized the results of the whole data with 15.0 kg barbell lifting motion. The 12.5 kg and 17.5 kg data were then used to compare the effects of different weights.

A total of 5 experimenters performed the lifting motion, and the height and weight of each experimenter were 170 cm-177 cm/65 kg-75 kg. As a result of motion capture, the joint angles of each experimenter showed little difference in the process of repetitive and slow lifting motions, but it was confirmed that they were operated in a specific range that was almost similar, and accordingly, the average data of the experimental values was used.

Fig. 2. Motion capture experimental marker setup.

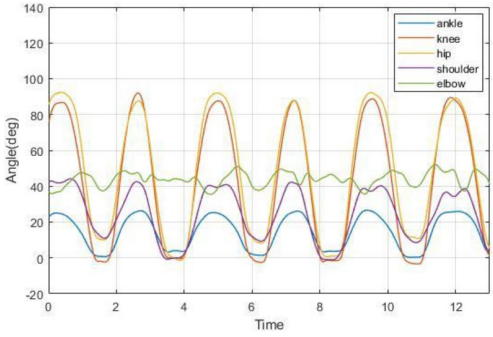

Fig. 3. Joint angle trajectory during the lifting motion.

Table 2. Maximum and minimum values of each joint trajectory.

	Max	*Min*
Ankle	27.0°	0.5°
Knee	91.7°	−3.0°
Hip	92.5°	−1.3°
Shoulder	40.7°	−1.4°
Elbow	48.5°	35.0°

Fig. 3 shows that each joint angle trajectory was repeated within a certain range during lifting. The hip and knee joints moved approximately 90 degrees, the ankle moved approximately 30 degrees, and the shoulder moved approximately 40 degrees. On the other hand, the elbow showed a fairly small movement of 13 degrees. The averages of the maximum and minimum values of each joint are expressed in Table 2. To implement this movement in the simulation, a smooth trajectory for generating human torque through PD (proportional–derivative) feedback was constructed based on Table 2.

3. WHOLE-BODY CONTROL BASED ASSISTANCE STRATEGY

3.1. Control system dynamics

In Section 2, a human lifting motion was expressed with 5 degrees of freedom. Complex model construction could describe human motions more accurately, but in practice, obtaining accurate model is not easy. It also causes difficulties in control. Meanwhile, the variation in the arm and forearm angle during lifting is not large enough to change the physical characteristics of the upper body above the hip joint. Therefore, as shown in Fig. 4, we assume the existing 6-link model on the left can be approximated as

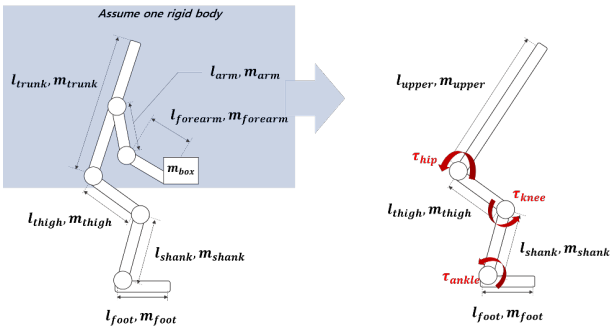

Fig. 4. Approximate box lifting model for control.

Fig. 5. Simulation model with exoskeleton.

a 4-link model. Finally, a simulation model is constructed as shown in Fig. 5.

As mentioned above, each link of the upper body was integrated into one rigid body, and the controller was constructed based on a 4-link configuration. In addition, to represent a human model wearing an exoskeleton, the human and exoskeleton were merged into one link in each part. The system control inputs are τ_{hip}, τ_{knee}, and τ_{ankle}, and the output values are the base IMU (inertial measurement unit) data and the encoder data of each joint.

3.2. WBC (whole-body control) framework

This section introduces a lifting assistance strategy based on whole-body control. Whole-body controllers for exoskeletons are formulated for a variety of tasks [12]. The variables are optimized to satisfy multiple tasks simultaneously. Then, the final torque is obtained through inverse dynamics. Fig. 6 shows the whole-body control framework block diagram.

The tasks for the lifting motion are divided into moving the COM (center of mass) with respect to the desired reference, maintaining the contact foot point, generating the contact force, preventing an excessive trunk angle, and obtaining the straight leg configuration. First, the COM motion consists of PD feedback on a reference trajectory. The x-direction reference is the initial value of the standing configuration for balancing, and the y-direction reference is determined simply by a motion capture experiment.

Once the PD feedback values for the trajectories in the x and y directions are obtained, a force reference is calculated based on them (2). F_r is the reference ground reaction force, $X_{cm,r}$ is the reference center of mass trajectory, X_{cm} is the current center of mass, and mg is the weight of the total mass. In (2)-(5), K_{pi} and K_{di} are the PD gains of each part.

$$F_r = mg(K_{p1}(X_{cm.r} - X_{cm}) + K_{1d}(\dot{X}_{cm.r} - \dot{X}_{cm}). \quad (2)$$

The foot contact task was formulated as (3). This means that each point of contact is maintained during the lifting operation. $x_{f,r}$ is the acceleration reference for each foot, and x_f is the current value of the foot position. Since there was no reference trajectory for the foot position during the lifting task, we set a value of 0 for the desired reference. In the same way, to prevent excessive movement of the trunk, another term was added to the cost function (4). $\ddot{\theta}_{trunk,r}$ is the reference trunk acceleration, and θ_{trunk} is the current trunk angle.

$$\ddot{x}_{f,r} = -K_{p2}x_f - K_{d2}\dot{x}_f, \quad (3)$$

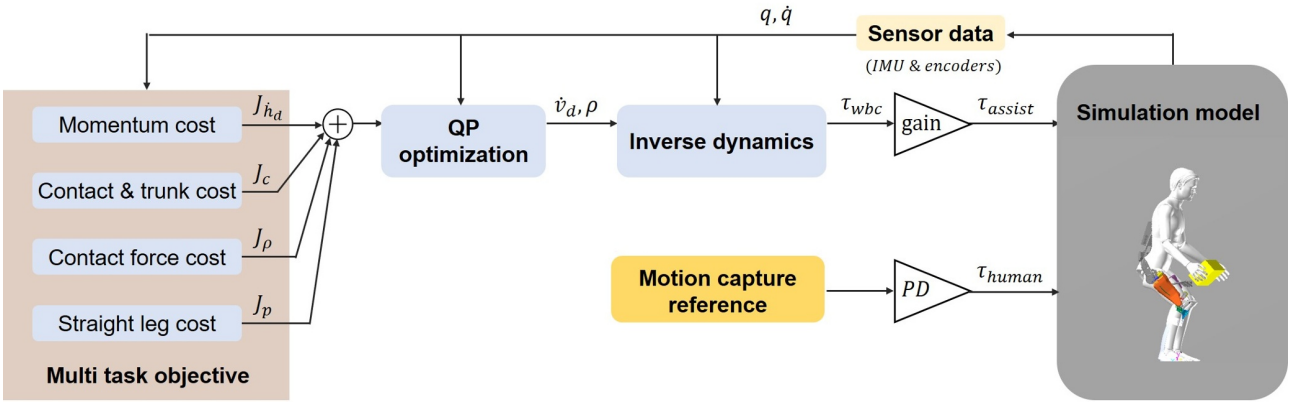

Fig. 6. Whole-body control framework for the exoskeleton model.

$$\ddot{\theta}_{trunk,r} = -K_{d3}\dot{\theta}_{trunk}. \quad (4)$$

On the other hand, a problem is encountered when performing the lifting motion only with the above tasks: the singularity problem. In general, for a legged robot walking, the singularity problem is not critical because the robot could avoid the fully extended leg configuration. However, at the end of the lifting motion, the legs are fully extended, and the singularity causes excessive torque. Authors of [20] proposed a solution through the straight leg control method, and based on this paper, a new term was now added to obtain the whole-body control bias solution.

Rather than directly controlling the height of the center of mass, we can place it in the null space of the desired leg configuration to keep the leg as straight as possible to avoid higher torque at the knee. When we do not specify a constraint on the vertical force, the whole-body controller can provide a wide variety of solutions to address each task.

To control the desired leg configuration while performing the existing task, the desired angle value is projected into the null space of the QP(quadratic programming). The desired angle to be projected is simply expressed as (5) as a feedback control law. q_{proj} is the predefined joint angle, $\dot{v}_{proj}$ is the corresponding acceleration of the joint and q is the current joint position. This formulation yields the straight leg cost term in (7). More details will be given in the next paragraph.

$$\dot{v}_{proj} = K_{p4}(q_{proj} - q) + K_{d4}v. \quad (5)$$

The final quadratic programming formula is shown in (6), and the optimization parameters are defined as $\dot{v}_d$ and ρ. $\dot{v}_d$ represents the desired joint accelerations, and ρ consists of the generalized forces. The meaning of each term in (6) is described in Table 3. There are total 13 parameters to be optimized (horizontal/vertical trunk position, trunk angle, joint angle of each leg, generalized foot force of left/right), and the number of constraints in the optimization process is determined in (7). 2 constraints at momentum cost, 5 $(= 4+1)$ constraints at contact trunk cost, 1 constraint at straight leg cost. Other terms are constructed for normalizing.

$$\begin{aligned}
&\min_{\rho,\dot{v}_d} J_h + J_J + J_\rho + J_p, \\
&\text{s.t. } A\dot{v}_d + \dot{A}v = W_g + W_{grf} \\
&\rho_{min} \le \rho \le \rho_{max}, \\
&\tau_{min} \le \tau \le \tau_{max}, \\
&\textit{Momentum cost}: \; J_h = ||P_h(A\dot{v}_d - B)||^2 \\
&\qquad\qquad \text{where } B = \begin{bmatrix} F_{ref} \\ 0_{3\times 1} \end{bmatrix} - \dot{A}v, \\
&\textit{Contact \& trunk cost}: \; J_J = ||P_J(J\dot{v}_d - p)||^2, \\
&\textit{Contact force cost}: \; J_\rho = ||P_\rho \rho||^2,
\end{aligned} \quad (6)$$

Table 3. Physical meaning of the variables.

v	generalized velocity
$\dot{v}_d$	desired generalized acceleration
A	centroidal momentum matrix
W_g	gravitational wrench
W_{grf}	wrench by ground reaction forces
ρ_{min}, ρ_{max}	minimum and maximum values of ρ
τ_{min}, τ_{max}	minimum and maximum values of τ

$$\begin{aligned}
&\textit{Straight leg cost}: \; J_p = ||(I - J_{task}^{+}J_{task})\dot{v}_{proj}||^2, \\
&\qquad\qquad \text{where } J_{task} = \begin{bmatrix} (SA)^T & J^T \end{bmatrix}^T.
\end{aligned} \quad (7)$$

Each term of the cost function is defined as in (7). p is the desired motion vector, and P_h, P_J, and P_J are the weight matrices that determine the importance of each term. To project the predefined acceleration into the null space of the QP, the term $J_p = ||(I - J_{task}^{+}J_{task})\dot{v}_{proj}||^2$ is added to the total cost function, as shown in (6) (the last term in the objective function). In the above formula, J of J_{task} is the cartesian motion objective jacobian which only contains contact jacobian in lifting operation case.

By adding the straight leg task term, the exoskeleton avoids the singularity problem. If a joint has a singularity configuration, a null space exists, and the predefined acceleration task succeeds. These QP bias solutions allow humans and exoskeletons to always stretch their knees 180 degrees, as straight as possible.

$$\tau = S(-J_c^T B\rho + M\dot{v}_d + b + g). \quad (8)$$

Finally, the torque value is obtained through inverse dynamics based on the optimized values $\dot{v}_d$ and ρ which are obtained through quadratic programming. Through the equation of motion obtained in (1), the inverse dynamics can be configured as in (8), and the torque value can be calculated by substituting $\dot{v}_d$ and ρ.

4. SIMULATION AND RESULTS

4.1. Simulation model and conditions

Simulations are conducted to verify the performance of the whole-body control based assisting strategy. A MATLAB Simulink controller is used, and it is implemented through cosimulation between MATLAB and the RecurDyn simulator. The control inputs to the exoskeleton are the hip, knee, and ankle torques, which are combined with the human-generated torques (described in Section 2). The output value is obtained from the IMU data of the base and the angle of each joint.

The box lifting operation is divided into a lowering operation and a raising operation. In the lowering process, it is not necessary to apply additional torque due to gravity acceleration. That is, the simulation is performed by applying assistance torque only during the lifting motion in

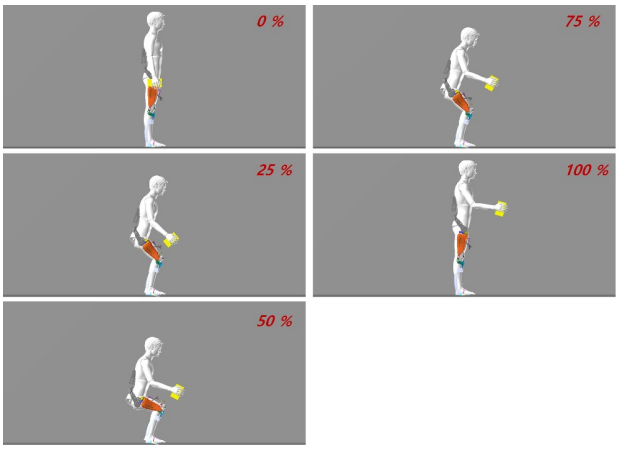

Fig. 7. Lifting simulation with a whole-body controller.

half phase of the cycle. Fig. 7 shows the simulation of the lifting operation. We obtained the results with various α, 0.0, 0.1, 0.2, 0.4 in the simulation, where α is the assistance gain(rate) of the whole-body controller.

4.2. Results

The simulation results were obtained as shown in Fig. 8. Since there is a limit to the torque value that the exoskeleton can produce, the obtained whole-body control torque was multiplied by a constant gain, denoted by α. As shown in the first row of Fig. 8, the hip torque and knee torque values decrease as the gain value increases. In the case of the ankle, it is difficult to compare the absolute torque value, but it can be seen that the variation has shifted to near 0.

As shown in Fig. 9, the assistance torque value of each joint can be seen in the lifting operation. As the α value increases, the amplitude value of each assistance torque increases, and we can see that the hip torque increases the most. However, in the second half, the torque value of the hip joint tends to decrease. Thus, it can be inferred that the knee joint and ankle joint torques are required more in a state close to standing. In the future, by designating different weights for each joint, the torque distribution can be obtained in a different form.

Next, the second row of Fig. 8 shows that the position of the x-direction center of mass, which can be considered a balancing index, is close to the center of the foot ($x = 0$). However, there is no significant difference in the y-direction according to the α value because the vertical trajectory is almost the same. To compare the used energy of the proposed controller, the accumulated power consumption of human torque is calculated. It decreases as the α value increases, and when the α value is 0.4, it is reduced to a maximum of 23.8%. Additionally, it is found that the problem of a singularity does not occur even in the fully extended configuration.

$$Mechanical\ cost\ of\ lifting = \frac{\int |\tau\omega| dt}{Mgd}. \tag{9}$$

In order to analyze the energy efficiency and stability, the mechanical cost of lifting and center of pressure (COP) during the lifting operation were analyzed. COP obtained the result as shown in Fig. 10 left one, and it can be seen that the value moved from the back to the front of the foot

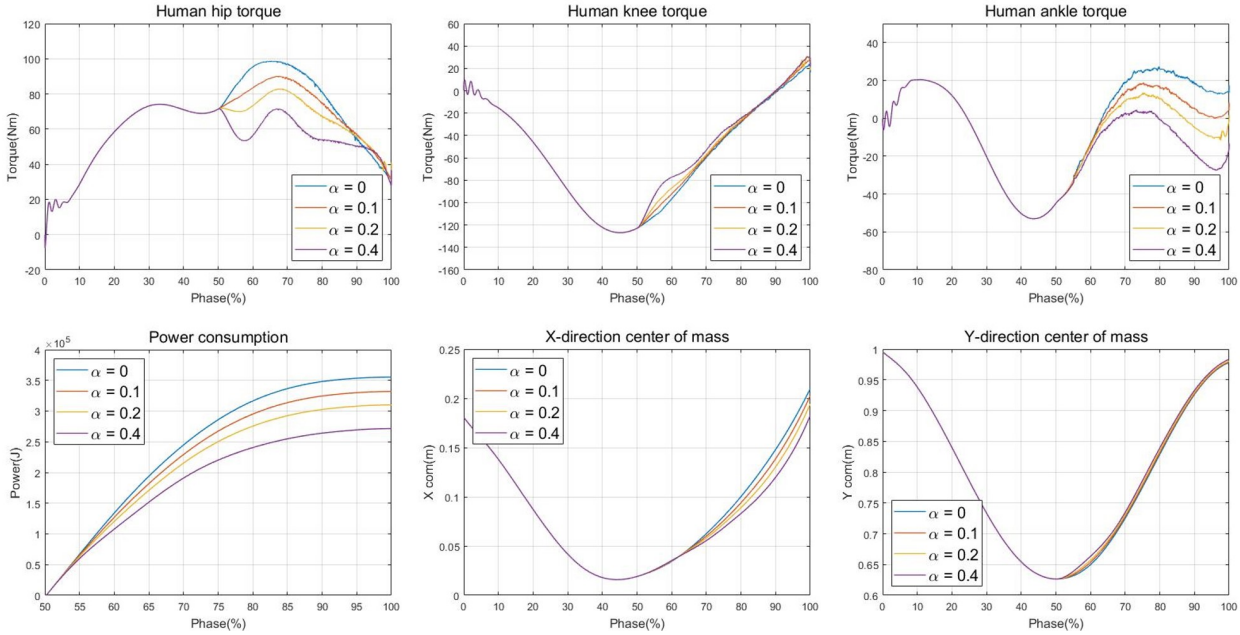

Fig. 8. Simulation results of the lifting motion. Human torque, center of mass and power consumption are compared. (α is the gain (rate) of the assistance).

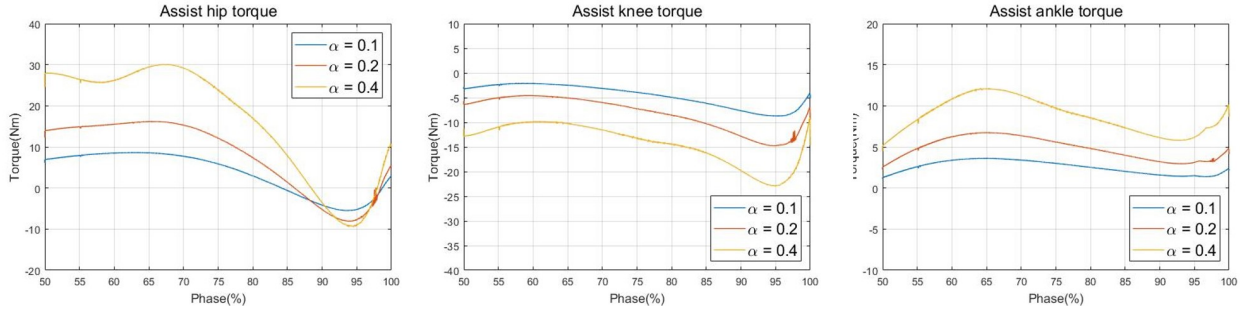

Fig. 9. Assistance torque value of the lifting simulation (τ_{wbc}). (α is the gain (rate) of the assistance).

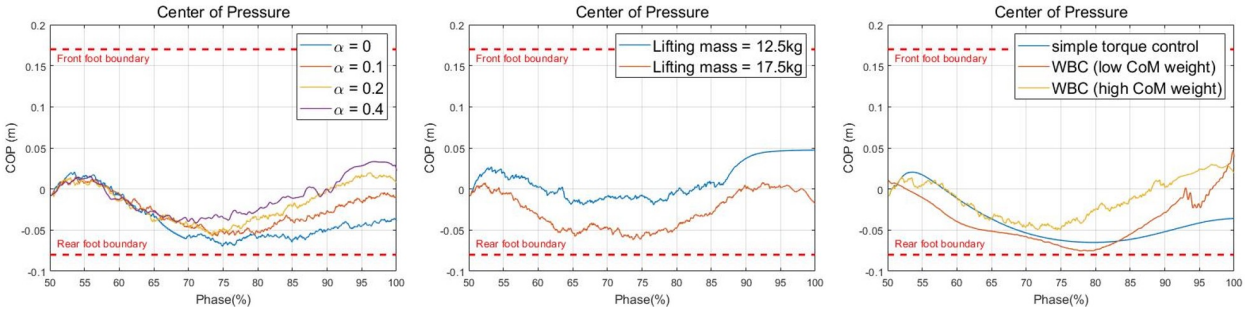

Fig. 10. Center of pressure during lifting simulation.

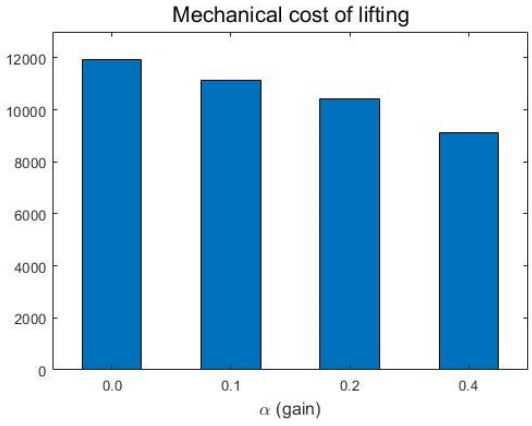

Fig. 11. Mechanical cost of lifting during simulation.

as α increased. When the alpha was 0.4, it was confirmed that the COP moved closer to the center of the foot. That is, as the assisting force increased, the stability increased. Next, an index called mechanical cost of lifting was newly defined for efficiency analysis as shown in (9). It was defined in a similar way to mechanical cost of transportation (MCOT), which is commonly used. d is the total lifting distance, Mg is the total weight, and the upper term $\int |\tau\omega| dt$ means energy consumption. When $\alpha = 0.4$, mechanical cost of lifting was reduced by up to 25% (Fig. 11).

In addition, the proposed controller was compared with another controller and different lifting weights. As shown in Fig. 10 second one, when the mass becomes heavy, the COP moves to the foot boundary even if assistance torque is added. This means that more gain or weight is needed to move the COP to the center of the foot. Next, in the last graph in Fig 10, we compare it to another controller that is simply torque control for the lifting. The comparative control strategy is constructed in the same way in the paper [22] obtaining the torque reference with $\tau = J^T F$. Here, the desired force was calculated to move the COP into the foot center and upright configuration. Also, there may be singularity issue, but when the system is close to the final configuration it decreases the assist force to zero. If you look at the comparison graph, you can see that the controller implemented as [22] can move the COP to inside the boundary. Meanwhile, in the case of whole-body controller, the movement amount of the COP can be adaptively adjusted according to the weight of the COM task. Additionally, the singularity problem was solved through a bias solution rather than simply making the assistance force zero, it can be considered as a more optimized solution. And the desired force was also obtained through whole dynamics rather than $\tau = J^T F$, therefore, more accurate force control is possible.

According to the analysis results of the two graphs, the proposed algorithm increases the efficiency as well as the stability during the lifting task. Additionally, when approaching a standing position, there is no singularity problem occurs, thus excessive torque could be avoided.

5. CONCLUSION

In this paper, two major tasks were performed. First, a motion capture experiment was performed to enable the simulation of human movement. Based on these results, a trajectory reference was created. A PD feedback torque was generated so that the human model could implement a lifting task in simulation, and it was assumed to be τ_{human}. Second, an assistance torque generation strategy applied by the exoskeleton was proposed based on whole-body control. A torque value was obtained that could simultaneously be used in various tasks in the lifting process.

Whole-body controller costs were roughly divided into momentum cost, contact & trunk costs, contact force cost and straight leg cost. In particular, due to the straight leg term we could overcome the singularity problems that occur in the fully extended configuration. As a result, it was verified that the lifting efficiency was increased without encountering the singularity problem, and the variation in the center of mass was also reduced. Additionally, we calculate the mechanical cost of lifting and COP during simulation. It was confirmed that the stability index, COP, moved toward the center of the foot, and the mechanical cost of lifting decreased as the assisting force increased. We also compared the controller with a simple torque controller and different lifting mass to verify its effectiveness.

In the future, we will conduct an experiment to apply the proposed algorithm to an actual exoskeleton. The platform development is almost complete, and it will be possible to control up to a 1 kHz bandwidth. Therefore, it seems that there is no major problem in applying the proposed algorithm. However, since interactions between humans and exoskeletons were not taken into account, this will be a problem that needs to be addressed. Also, in order to verify the proposed controller, we plan to conduct a experiments with more subjects.

CONFLICT OF INTEREST

The authors should ensure that there is no potential conflict of interest possibly influencing the interpretation of data in the paper. Also, the authors who have no relevant financial interests or private connections should provide a statement indicating that they have no interests related to the material in the manuscript. For example, "The authors declare that there is no competing financial interest or personal relationship that could have appeared to influence the work reported in this paper."

REFERENCES

[1] B. Penzlin, M. E. Fincan, Y. Li, L. Ji, S. Leonhardt, and C. Ngo, "Design and analysis of a clutched parallel elastic actuator," *Actuators*, vol. 8, no. 3, 67, 2019.

[2] M. B. Näf, A. S. Koopman, S. Baltrusch, C. Rodriguez-Guerrero, B. Vanderborght, and D. Lefeber, "Passive back support exoskeleton improves range of motion using flexible beams," *Frontiers in Robotics and AI*, vol. 5, 72, 2018.

[3] M. Abdoli-E, M. J. Agnew, and J. M. Stevenson. "An on-body personal lift augmentation device (PLAD) reduces EMG amplitude of erectorspinae during lifting tasks," *Clinical Biomechanics*, vol. 21, no. 5, pp. 456–465, 2006.

[4] B. H. Whitfield, P. A. Costigan, J. M. Stevenson, and C. L. Smalllman, "Effect of an on-body ergonomic aid on oxygen consumption during a repetitive lifting task," *International Journal of Industrial Ergonomics*, vol. 44, no. 1, pp. 39–44, 2014.

[5] C. A. Lotz, M. J. Agnew, A. A. Godwin, and J. M. Stevenson, "The effect of an on-body personal lift assist device (PLAD) on fatigue during a repetitive lifting task," *Journal of Electromyography and Kinesiology*, vol. 19, no. 2, pp. 331–340, 2009.

[6] R. K. P. S. Ranaweera, R. A. R. C. Gopura, T. S. S. Jayawardena, and G. K. I. Mann, "Development of a passively powered knee exoskeleton for squat lifting," *Journal of Robotics, Networking and Artificial Life*, vol. 5, no. 1, pp. 45–51, 2018.

[7] S. Mohri, H. Inose, H. Arakawa, K. Yokoyama, Y. Yamada, I. Kikutani, and T. Nakamura, "Development of non-rotating joint drive type gastrocnemius-reinforcing power assist suit for squat lifting," *Proc. of IEEE International Conference on Advanced Intelligent Mechatronics (AIM)*, IEEE, pp. 851–856, 2017.

[8] W. Wei, S. Zha, Y. Xia, J. Gu, and X. Lin, "A hip active assisted exoskeleton that assists the semi-squat lifting," *Applied Sciences*, vol. 10, no. 7, 2424, 2020.

[9] S. M. Tahamipour-Z, S. K. H. Sani, A/ Akbarzadeh, and I. Kardan, "An assistive strategy for compliantly actuated exoskeletons using non-linear model predictive control method," *Iranian Conference on Electrical Engineering (ICEE)*, IEEE, pp. 982–987, 2018.

[10] W. M. dos Santos and A. A. G. Siqueira, "Optimal impedance via model predictive control for robot-aided rehabilitation," *Control Engineering Practice*, vol. 93, 104177, 2019.

[11] S. Luo, G. Androwis, S. Adamovich, H. Su, E. Nunez, and X. Zhou, "Reinforcement learning and control of a lower extremity exoskeleton for squat assistance," *Frontiers in Robotics and AI*, vol. 8, 702845, 2021.

[12] T. Koolen, S. Bertrand, G. Thomas, T. de Boer, T. Wu, J. Smith, J. Englsberger, and J. Pratt, "Design of a momentum-based control framework and application to the humanoid robot atlas," *International Journal of Humanoid Robotics*, vol. 13, no. 1, 1650007, 2016.

[13] D. Kim, S. J. Jorgensen, J. Lee, J. Ahn, J. Luo, and L. Sentis, "Dynamic locomotion for passive-ankle biped robots and humanoids using whole-body locomotion control," *The Interna-tional Journal of Robotics Research*, vol. 39, no. 8, pp. 936–956, 2020.

[14] B. Henze, A. Dietrich, and C. Ott, "An approach to combine balancing with hierarchical whole-body control for legged humanoid robots," *IEEE Robotics and Automation Letters*, vol. 1, no. 2, pp. 700–707, 2015.

[15] D. Kim, Y. Zhao, G. Thomas, B. R. Fernandez, and L. Sentis, "Stabilizing series-elastic point-foot bipeds using whole-body operational space control," *IEEE Transactions on Robotics*, vol. 32, no. 6, pp. 1362–1379, 2016.

[16] D. Kim, J. di Carlo, B. Katz, G. Bledt, and S. Kim, "Highly dynamic quadruped locomotion via whole-body impulse control and model predictive control," arXiv preprint arXiv:1909.06586, 2019.

[17] A. Tözeren, *Human Body Dynamics: Classical Mechanics and Human Movement*, Springer Science & Business Media, 1999.

[18] H. Inose, S. Mohri, Y. Yamada, T. Nakamura, K. Yokoyama, and I. Kikutani, "Development of a light weight power-assist suit using pneumatic artificial muscles and balloon-amplification mechanism," *Proc. of 14th International Conference on Control, Automation, Robotics and Vision (ICARCV)*, IEEE, pp. 1–6, 2016.

[19] R. Drillis, R. Contini, and M. Bluestein. "Body segment parameters," *Artificiallimbs*, vol. 8, no. 1, pp. 44–66, 1964.

[20] R. J. Griffin, G. Wiedebach, S. Bertrand, A. Leonessa, and J. Pratt, "Straight-leg walking through underconstrained whole-body control," *Proc. of IEEE International Conference on Robotics and Automation (ICRA)*, IEEE, pp. 5747–5754, 2018.

[21] F. L. Moro, N. Iannacci, G. Legnani, and L. M. Tosatti, "A passivity-based concurrent whole-body control (cWBC) of persistently interacting human-exoskeleton systems," arXiv preprint arXiv:1708.02816, 2017.

[22] M. Jeong, H. Woo, and K. Kong, "A study on weight support and balance control method for assisting squat movement with a wearable robot, angel-suit," *International Journal of Control, Automation, and Systems*, vol. 18, no. 1, pp. 114-123, 2020.

Jeonguk Kang received his B.S. and M.S. degrees in mechanical engineering from the Korea Advanced Institute of Science and Technology (KAIST), Daejeon, Korea, in 2018 and 2020, respectively. He is currently pursuing a Ph.D. degree in mechanical engineering at KAIST. His research interests include legged robots and state estimation.

Donghyun Kim received his B.S. and M.S. degrees in mechanical engineering from the Korea Advanced Institute of Science and Technology (KAIST), Daejeon, Korea, in 2016 and 2018, respectively. He is currently pursuing a Ph.D. degree in mechanical engineering at KAIST. His research interests include legged robots, whole-body control, pneumatic actuators, and their control.

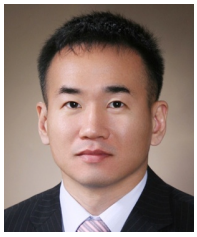

Hyun-Joon Chung received his B.E. degree in mechatronics engineering from Chungnam National University, Daejeon, Korea, in 1996 and his M.S. and Ph.D. degrees in mechanical engineering from the University of Iowa, Iowa City, USA, in 2005 and 2009, respectively. He was a research assistant and postdoctoral research scholar at the Center for Computer Aided Design from 2005 to 2015. He joined the Korea Institute of Robotics and Technology Convergence as a senior researcher in 2015. He is currently a principal researcher and the head of the AI Robotics Center at the Korea Institute of Robotics and Technology Convergence. He serves as a general affairs director of the Field Robot Society in Korea. His research interests include dynamics and control, optimization algorithms, computational decision making, modeling and simulation, and robotics.

Kwang-Woo Jeon received his B.E. and M.S. degrees in mechanical design engineering from Hanbat National University, Daejeon, Korea, in 2011 and 2013, respectively. He was an Assistant Researcher of research division of Korea Institute of Robot and technology convergence, from 2012 to 2013. And, he joined the HanKuk fiber as a Senior Researcher from 2014 to 2015. He joined the Korea Institute of Robotics and Technology Convergence as a Senior Researcher in 2015. He is currently a Senior Researcher of AI Robotics Center in Korea Institute of Robotics and Technology Convergence. His research interests include design of rehabilitation robot and human interaction robot.

Kyung-Soo Kim received his B.S., M.S., and Ph.D. degrees in mechanical engineering from the Korea Advanced Institute of Science and Technology (KAIST), Daejeon, Korea, in 1993, 1995, and 1999, respectively. He was a chief researcher with LG Electronics, Inc., from 1999 to 2003 and a DVD group manager with STMicroelectronics Company, Ltd., from 2003 to 2005. In 2005, he joined the Department of Mechanical Engineering, Korea Polytechnic University, Siheung, Korea, as a faculty member. Since 2007, he has been with the Department of Mechanical Engineering at KAIST. He serves as an associate editor of Automatica and the Journal of Mechanical Science and Technology. His research interests include control theory, electric vehicles, and autonomous vehicles.